Sensitivity Analysis in the Design of a Packed-Bed Reactor for a Chemical Looping Combustion Process

Giuseppe Diglio, Piero Bareschino, Erasmo Mancusi*, Francesco Pepe

Dipartimento di Ingegneria, Università degli Studi del Sannio, Piazza Roma, 21 – 82100 Benevento
mancusi@unisannio.it

Chemical Looping Combustion (CLC) is a cyclic unmixed combustion technology that allows the inherent separation of CO_2. In CLC, fuel and oxygen are contacted via an intermediate oxygen carrier, usually a metal oxide capable of being alternately oxidized and reduced. In this way direct contact between fuel and combustion air is avoided, thus producing an N_2-free, CO_2 rich stream. Different reactor typologies and layouts have been proposed for CLC: among them, packed-bed reactors are currently under the spotlight since they can be more easily operated at high pressure with respect to fluidized bed reactors and, moreover, there is no need for a gas/solid separation step in order to ensure that no fines are sent to the downstream gas turbine. One of the drawbacks in using packed-bed reactors is that several reactors in parallel must be used to achieve a continuous supply of a high temperature gaseous stream for the downstream gas turbine.
In the present work a one-dimensional pseudo-homogeneous model is used to carry out a numerical analysis of chemical looping combustion process for heat production, using a Cu-based oxygen carrier and methane as fuel. By means of numerical simulations, the effect of main operating parameters such as inlet temperature and time length of each phase on the process performances is investigated.

1. Introduction

Carbon dioxide (CO_2) is one of the most significant contributors to greenhouse effect and its emissions from stationary sources are still increasing (Chou et al., 2013). Chemical Looping Combustion (CLC) is a Carbon Capture and Sequestration (CCS) technologies for the containment of CO_2 emission from stationary sources: CLC is a cyclic unmixed combustion process, whose core element is an Oxygen Carrier (OC), a metallic solid alternatively oxidized and reduced: the net effect is the conversion of fuel and oxygen to an N_2-free, H_2O and CO_2 rich gaseous stream, that can be easily purified (Diglio et al., 2016a).
Interconnected fluidized bed systems were widely investigated for CLC (Diglio et al., 2017b); recently, packed-beds were proposed as a feasible alternative to fluidized beds given that they are more easily to pressurize, and there is no need for a gas/solid separation step (Noorman et al., 2007).
Depending on the OC/fuel pair (Diglio et al., 2017a), at least three steps can be individuated operating CLC process in a fixed bed, namely Oxidation phase (OP), Heat Removal phase (HR) and Reduction phase (RP). During the first step, the OC is exothermically oxidized by feeding an air stream to the reactor. At the end of OP almost all of the produced heat is still inside the reactor, due to the amount of solid inert in the OC; consequently, during the second step, air can be fed to reactor to produce a high temperature stream for turbine expansion; finally, over the last step, the catalyst is reduced by feeding fuel to the reactor.
When Cu-based OC and CH_4 as fuel are used both the OP and the RP are exothermic and therefore a further HR step can occur after the RP, generating an extra-hot gas stream for turbine expansion. In this work the performances of a packed-bed reactor operated under CLC conditions when Cu and CH_4 are used as OC and fuel, respectively, will be numerically investigated.

2. Mathematical model

2.1 Reaction kinetic network

The reaction mechanisms proposed by Garcia-Labìano et al. (2004) were used to describe the reactions between Cu/CuO and both methane and oxygen. The adopted global kinetic scheme is reported in Table1, with associated standard enthalpies of reactions. The catalyst in its reduced form is oxidized by air through reaction (R1), while the global reduction process is given by reaction (R2).

Table 1: kinetic scheme and associated standard enthalpies of reactions.

Reaction	ΔH^0, kJ·mol^{-1}	
$2Cu + O_2 \rightarrow 2CuO$	-312	R1
$4CuO + CH_4 \rightarrow 4Cu + CO_2 + 2H_2O$	-178	R2

As reported by Abad et al. (2007), the reaction rate of Cu-based oxygen carrier with fuel gas or with air can be expressed by means of the shrinking-core mode for plate-like geometry under chemical reaction control:

$$\frac{dX_j}{dt} = \frac{1}{\tau_j} \tag{1}$$

$$\tau_j = \frac{\rho_m \cdot L_k}{b_j \cdot K_j \cdot C_i^m} \tag{2}$$

$$r_j = \frac{\varepsilon_s \cdot \varepsilon_p \cdot \rho_s \cdot w_{act}^0 \cdot \eta_j}{M_k} \cdot \frac{dX_j}{dt} \tag{3}$$

where X is the solid conversion, t is the time (s), τ is the reaction time (s), ρ_m and ρ_s are the molar and solid density (mol·m^{-3}), respectively, L_k is the layer thickness of reacting solid (m), b is the stoichiometric coefficient, K_j is the Arrhenius exponential constant of reaction j (mol·m^{-3}·s^{-1}), C is the gas specie concentration (mol·m^{-3}), ε_s and ε_p are the void fractions of the solid and of the particle, respectively, w_{act}^0 is the initial mass fraction of active phase on the OC, M is the molecular weight (kg·mol^{-1}), η is the reaction effectiveness and m is the reaction order; the subscripts i, k and j are for the gas species (CH_4, H_2O, CO_2, O_2 and N_2), the solid species (Cu and CuO) and chemical reaction index (oxidation and reduction), respectively.
The kinetic data given by Garcia-Labìano at al. (2004) are reported in Table 2.

Table 2: kinetic data.

	$K_{0,j}$, mol^{1-n}·m^{3n-2}·s^{-1}	E_j J·mol^{-1}	m	η	L_k, m	ρm, mol·m^{-3}
CH_4	$4.5 \cdot 10^{-4}$	$60 \cdot 10^3$	0.4	0.36	$4.0 \cdot 10^{-10}$	80402
O_2	$4.7 \cdot 10^{-4}$	$15 \cdot 10^3$	1.0	0.85	$2.3 \cdot 10^{-10}$	140252

2.2 Mass and energy balances

In this work geometrical characteristics of reactor were taken from Noorman et al. (2007), as those of an industrial application; in such a reactor, when Cu-based oxygen carrier is used, there are no radial temperature or concentration gradients and heat transfer between gas and solid phases can be neglected. As a consequence, a 1D pseudo-homogeneous model can be used to investigate the dynamic behaviour of adiabatic packed-bed reactor operated under CLC conditions.
In particular, oxidation and reduction steps were modelled by means of mass and enthalpy balances for each species and a global momentum balance (Ergun equation). The resulting equations with corresponding initial and boundary conditions are reported in Table 3, where z is the axial spatial variable (m), L is the reactor length (m), u_g is the gas superficial velocity (m·s^{-1}), ε_g is the gas voidage, D_{ax} is the effective axial dispersion (m^2·s^{-1}), ρ_g is the gas density, T is the temperature (K), cp_g and cp_s are the gas and solid heat capacity (J·kg^{-1}·K^{-1}), respectively, λ_{ax} is the effective heat dispersion coefficient (W·m^{-1}·K^{-1}), P is the pressure (Pa), d_p is the particle diameter (m), μ_g is the gas dynamic viscosity (Pa·s), λ_g is the gas thermal conductivity (W·m^{-1}·K^{-1}), λ_e^0 is the static contribution to effective axial dispersion the value of which is 0.01 W·m^{-1}·K^{-1} (Yagi and Wakao, 1959), Re is the Reynolds number, Pr is the Prandtl number, Sc is the Schmidt number and the subscript in is referred to inlet conditions.

Table 3: governing equations.

Gas phase mass balance	$\varepsilon_g \dfrac{\partial C_i}{\partial t} + u_g \dfrac{\partial C_i}{\partial z} = \varepsilon_g \dfrac{\partial}{\partial z}\left(D_{ax}\dfrac{\partial C_i}{\partial z}\right) + \varepsilon_g \dfrac{r_j}{b_j}$
Solid phase mass balance	$\dfrac{\partial C_k}{\partial t} = r_j$
Energy balance	$\left(\varepsilon_g \rho_g cp_g + \varepsilon_s \rho_s cp_s\right)\dfrac{\partial T}{\partial t} + \left(\varepsilon_g \rho_g cp_g u_g\right)\dfrac{\partial T}{\partial z} = \varepsilon_g \dfrac{\partial}{\partial z}\left(\lambda_{ax}\dfrac{\partial T}{\partial z}\right) + \varepsilon_g r_J(-\Delta H_J)$
Momentum balance	$-\dfrac{\partial P}{\partial Z} = 150\dfrac{\mu_g \cdot u_g}{d_p^{\,2}}\dfrac{(1-\varepsilon_g)^2}{\varepsilon_g^{\,3}} + 1.75\dfrac{\rho_g \cdot u_g^{\,2}}{d_p}\dfrac{(1-\varepsilon_g)}{\varepsilon_g^{\,3}}$
Boundary conditions	$\dfrac{\partial C_i(0,t)}{\partial z} = \dfrac{u_g}{\varepsilon_g D_{ax}}\left(C_i(0,t)-C_{i,in}\right),\quad \dfrac{\partial C_i(L,t)}{\partial z}=0$ $\dfrac{\partial T(0,t)}{\partial z} = \dfrac{u_g cp_g \rho_g}{\varepsilon_g \lambda_{ax}}\left(T(0,t)-T_{in}\right),\quad \dfrac{\partial T(L,t)}{\partial z}=0$
Additional equations	$D_{ax} = \left(\dfrac{0.73}{Re\cdot Sc} + \dfrac{0.5}{\varepsilon_g + \dfrac{9.7\varepsilon_g^{\,2}}{Re\cdot Sc}}\right)u_g d_p$ $\lambda_{ax} = \lambda_e^0 + 0.7 Pr\cdot Re\cdot \lambda_g$

The correlation of Edwards and Richardson (1968) was used to evaluate D_{ax}, while the expression proposed by Yagi and Wakao (1959) was taken into account for λ_{ax}. Further details on the mathematical model and on the mathematical expression of the cyclic nature of CLC process can be found in Diglio et al. (2016b).

3. Results and discussion

3.1 Model validation

Model parameters were adapted to the system described by Noorman et al. (2007), as reported in Table 4, and a comparison between calculated and experimental literature data (Noorman et al., 2007) was performed to validate the mathematical model. Figure 1 reports temperature (A), solid conversion (B) and O_2 molar fraction (C) along axial coordinate of reactor at different times: noteworthy, the model is able to describe both quantitatively and qualitatively literature data.

Table 4: parameters used for model validation.

Parameter	Value
P_{in}, Pa	$3\cdot 10^5$
T_{in}, K	873
L, m	1.0
cp_s, $J\cdot kg\cdot K^{-1}$	1080
ρ_s, $kg\cdot m^{-3}$	3000
d_p, m	$2\cdot 10^{-3}$
w_{act}^0	0.20
ε_s	0.40
ε_p	0.57

After proper model validation, the same parameters reported in Table 4 were used to evaluate the dynamic behaviour of the fixed-bed. Furthermore, T_{in} was increased, as detailed in the following section, in order to set the best operating conditions. The gas superficial velocity was set at $0.96\ m\cdot s^{-1}$ during OP, at $0.17\ m\cdot s^{-1}$ during RP, and at $1.54\ m\cdot s^{-1}$ during HR.
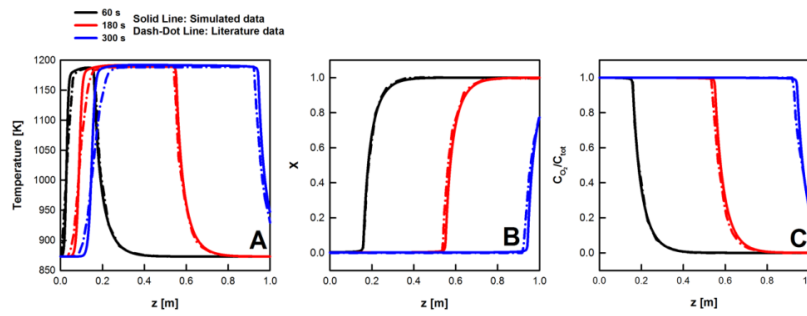
Figure 1: spatial temperature (A), solid conversion degree (B) and O_2 molar fraction (C) profiles at different times; solid lines represent simulated data, dash-dot lines denotes literature data.

3.2 Initial temperature of the bed

Initial temperature of the bed, T_0, should be nor too high neither too low: indeed, on the one hand, if T_0 is too high, the maximum temperature reached in the reactor could cause irreversible catalyst deactivation; on the other hand, if T_0 is too low, reduction reaction could be not triggered. A good compromise is to set T_0 around 1000 K, which leads to a maximum temperature in the reactor, according to Eq(4), equal to about 1320 K and 1200 K during OP and RP, respectively. Such values are not only below the melting point of Cu-based oxygen carrier ($\approx$1400 K: Adànez at al., 2012), but also values at which the catalyst is still able to work, as reported by Adànez (Adànez et al., 2012); moreover, the chosen value of T_0 is sufficiently close to the threshold temperature over which reduction reaction rate significantly increases (Garcia-Labìano at al., 2004).

$$\Delta T = \frac{-\Delta H_j}{\dfrac{cp_s \cdot M_{act}}{w_{act}^0 \cdot b_j} + \dfrac{cp_g \cdot M_{rea}}{w_{rea}^{in}}} \qquad (4)$$

where ΔH_j is the enthalpy of reaction j (J·mol^{-1}), M_{act} and M_{rea} are the molecular weight of solid active phase on the OC and of reacting gas, respectively, and w_{rea}^{in} is the inlet mass fraction of reacting gas.

To avoid discontinuity between initial temperature of the bed and feed temperature, T_{in} was set to 1000 K too.

3.3 Length of Oxidation, Reduction and Heat Removal phases

The process is started when the OC contained in the reactor is in its reduced form (Cu). Figure 2 reports: temperature (A) and conversion degree (B) spatial profiles at different times, and O_2 molar fraction time profile at reactor exit (C). The exothermic oxidation reaction (R1) releases a relevant amount of heat, thus increasing bed temperature and two "fronts" (a reaction one and a thermal one) propagate through the packed-bed reactor with different velocities (Noorman et al., 2007). Figure 2C shows that O_2 concentration at the reactor exit reaches its initial value after about 316 s, as soon reactor exit section reaches the maximum temperature achieved in the bed (see Fig. 2A): this means that after such an amount of time the whole OC is oxidized (see Figure 2B, solid conversion degree is 1 everywhere). Extending the OP for more than 316 s has the detrimental effect to further propagate the thermal front (see the curve relative to t=350 s in Figure 2A), cooling the reactor.

After OP, a HR step is started, during which air is still fed to the reactor in order to remove produced heat for subsequent power generation in a gas turbine system. The length of HR phase must be chosen in order to avoid that the temperature of the produced hot air stream drops below the specific optimal value for the gas turbine (1273 K – 1473 K: Noorman et al., 2007); Figure 3A reports temperature profile at the outlet of the reactor during both OP and HR: by inspecting this figure it is clear that after the OP (blue zone), an hot air stream at approximatively constant temperature is produced until t=1919 s; after that, temperature drops below 1300 K; as a consequence, a HR length of 1603 s (from t=316 s to t=1919 s) must be chosen. Before starting the reduction phase, a Purge Phase (PP) with nitrogen is carried out (filled zone in Figure 3A) in order to avoid the formation of potentially explosive O_2-H_2 gas mixture: as shown in Figure 3B, that reports temperature spatial profile at different times during the first HR and the subsequent purge step, the PP is extended until to restore the initial spatial temperature profile, i.e. for further 63 s (from 1919 s to 1982 s); it is fundamental to have a T_0 uniform spatial temperature profile before starting the RP, otherwise bed temperature could reach unacceptably high values. As highlighted in Figure 3B, at the end of purge phase the reactor zone close to the exit is at temperature higher than T_0: this small amount of heat stored in the bed

does not affects temperature profile of subsequent reduction phase, since it will be pushed out in the very first time instants of RP.

Figure 4 reports outlet gas molar fraction (A) and spatial temperature profiles (B) at different times during the first RP. Only H_2O and CO_2 leave the reactor during RP; unconverted CH_4 starts to be detected at reactor exit after approximatively 150 s (Figure 4A) and reaches about half of its inlet value after 195 s, a time at which all of the catalyst is completely reduced, since y_{H2O} and y_{CO2} quickly decrease. Figure 4B shows the effect of exothermic reduction reactions, also highlighting that the maximum temperature reaches reactor outlet at about 195 s; from this time on, there will only be a bed cooling if the RP is protracted (see t=250 s in Figure 4B). Likewise after OP, after RP a HR step can occur: by feeding N_2, this further HR is extended up to restore the initial spatial temperature profile, *i.e.* for 1023 s.
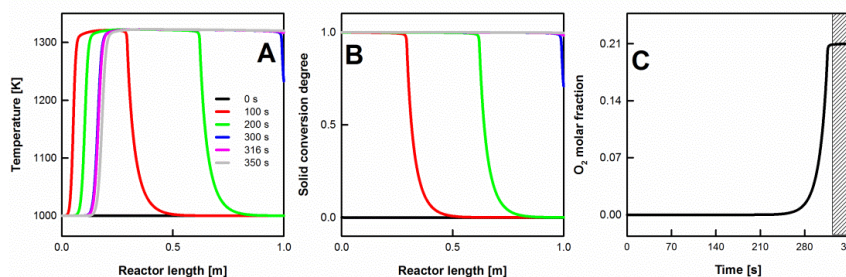

Figure 2: spatial temperature (A) and solid conversion (B) degree profiles at different times and O_2 molar fraction at the reactor exit (C) during the first oxidation phase.
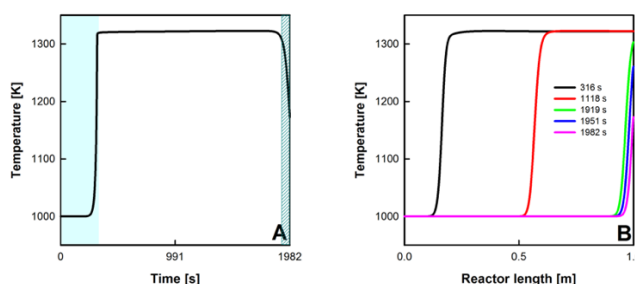

Figure 3: temperature at the reactor exit (A) during the first oxidation (in blue), heat removal and purge phases (filled zone), and spatial temperature profiles (B) at different times during the first HR and PP phases.
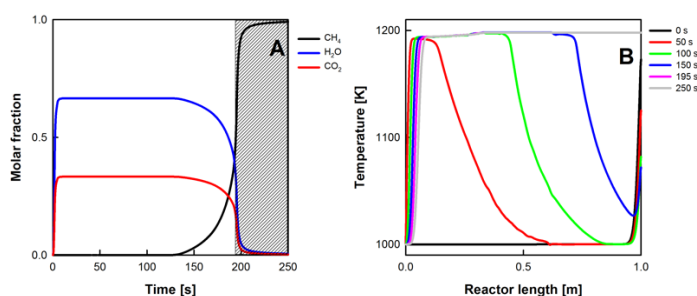

Figure 4: outlet gas molar fraction (A) and spatial temperature profiles at different times (B) during the first RP.

3.4 Cyclic operation

In this section a sequence of OP, HR, PP, RP and HR is numerically simulated, fixing the time lengths of each one of the above phases at the values previously estimated, and therefore with an overall length of a whole cycle of 3200 s. Figure 5 reports outlet temperature of a generic cycle when regime is attained (*i.e.* after 3-4 cycles): it is remarkable that two hot gas streams at about 1320 K and 1200 K are obtained during the two HR, after OP and RP, respectively.
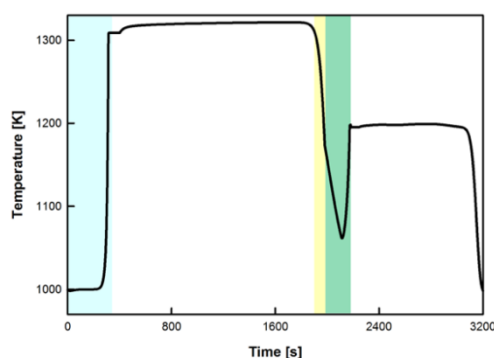
Figure 5: outlet temperature during a generic cycle when regime is reached (OP is blue zone, HR are white zones, PP is yellow zone and RP is green zone) .

4. Conclusion

A CLC process in a packed-bed reactor using CH_4 as fuel and Cu-based OC was numerically investigated by means of 1D pseudo-homogeneous model, validated by comparison with experimental data available in literature. The study results revealed a strong influence of the initial temperature and the time length of each phase. In particular, it was shown that the initial bed temperature (T_0) should be set at about 1000 K in order to achieve the threshold ignition value for reduction reaction; moreover, it was found that the Oxidation Phase (OP) should be extended until the fed value of O_2 and the maximum temperature reached in the bed are detected at reactor exit, i.e t_{OP}=316 s for the case studied; after OP, the Heat Removal (HR) phase should be protracted until outlet temperature drops below 1300 K, *i.e.* $t_{HR,OP}$=1603 s in the conditions simulated; the subsequent Purge Phase (PP) should be run unto to restore T_0 uniform spatial profile (t_{PP} =63 s), otherwise the temperature could reach unacceptable values in the subsequent Reduction Phase (RP), which should be extended until the achieved maximum temperature is detected at reactor outlet (t_{RP}=195 s); after RP, a further HR with N_2 should be extended until a uniform T_0 spatial profile is restored ($t_{HR,RP}$=1023 s). Future developments of this work will include detailed analysis of reactors network operated under the above described conditions in order to achieve the continuous production of a hot gas stream in both HR phases.

Reference

Abad A., Adànez J., Garcìa-Labiano F., de Diego L.F., Gayàn P., Celaya J., 2007, Mapping the range of operational conditions for Cu-, Fe-, and Ni-based oxygen carriers in chemical-looping combustion, Chem. Eng. Sci. 62, 533-549.

Adànez J., Abad A., Garcìa-Labiano F., Gayàn P., de Diego L.F., 2012, Progress in Chemical-Looping Combustion and Reforming technologies, Progr. Energ. Combust. 38, 215-82.

Chou C.T., Chen F.H., Huang Y.J., Yang H.S., 2013, Carbon Dioxide Capture and Hydrogen Purification from Synthesis Gas by Pressure Swing Adsorption, Chemical Engineering Transaction 32, 1855-60

Diglio G. Bareschino P., Mancusi E., Pepe F., 2016a, Chemical Looping Reforming: Impact on the Performances due to Carbon Fouling on Catalyst, Comput. Aided Chem. Eng. 38, 229-34.

Diglio G., Bareschino P., Mancusi E., Pepe F., 2016b, Simulation of hydrogen production through chemical looping reforming process in a packed-bed reactor, Chem. Eng. Res. Des. 105, 137-51.

Diglio G., Bareschino P., Mancusi E., Pepe F., 2017a, Numerical Assessment of the Effects of Carbon Deposition and Oxidation on Chemical Looping Combustion in a Packed-bed Reactor, Chem. Eng. Sci. 160, 86-96.

Diglio G., Bareschino P., Solimene R., Mancusi E., Pepe F., Salatino P. 2017b, Numerical Simulation of Hydrogen Production by Chemical Looping Reforming in a Dual Fluidized Bed Reactor, Powder Technol., in Press, http://dx.doi.org./10.1016/j.powtec.2016.12.051.

Edwards M.F. and Richardson J.F., 1968, Gas dispersion in packed beds, Chem. Eng. Sci. 23, 109-123.

Garcia-Labìano F., de Diego L.F., Adànez J., Abad A., Gayàn P., 2004, Reduction and oxidation kinetics of copper-based oxygen carrier prepared by impregnation for chemical-looping combustion, Ind. Eng. Chem. Res. 43, 8168-77.

Noorman S., van Sint Annaland M., Kuipers H., 2007, Packed Bed Reactor Technology for Chemical-Looping Combustion, Ind. Eng. Chem. Res. 46, 4212-20.

Yagi S., Wakao N., 1959, Heat and mass transfer from wall to fluid in packed beds, AIChE J. 5, 79-85.